Astron. Astrophys. 361, 841–849 (2000)

ASTRONOMY
AND
ASTROPHYSICS

Characterizing bar structures: application to NGC 1300, NGC 7479 and NGC 7723

J.A.L. Aguerri[1,2], **C. Muñoz-Tuñón**[1], **A.M. Varela**[1], **and M. Prieto**[1]

[1] Instituto de Astrofísica de Canarias, 38200 La Laguna, Tenerife, Spain
[2] Astronomisches Institut der Universitat Basel, Venusstrasse 7, 4102 Binningen, Switzerland (jalfonso@astro.unibas.ch)

Received 16 December 1999 / Accepted 30 May 2000

Abstract. Detailed surface photometry has been carried out for three barred galaxies with use of high resolution CCD broad-band images in the B, V and I bands. Using azimuthal luminosity profiles and their decomposition into Fourier Series, the structural parameters (length and strength) of the bars in the three galaxies have been obtained. We have also inferred the corotation radii (CR) using information available in the $B-I$ and $B-V$ colour index profiles. The regions selected for the CR were the ends of the bars, or a little further out and with an older stellar population than the su rrounding regions. The resulting values, $R_{\rm CR} \sim 100'' \pm 10''$ for NGC 1300, $R_{\rm CR} \sim 63''$ for NGC 7479 and $R_{\rm CR} \sim 23''$ for NGC 7723, are in agreement with those previously reported in the literature. This demonstrates the utility of accurate photometry for this type of observation.

Key words: galaxies: individual: NGC 1300, NGC 7479, NGC 7723 – galaxies: spiral – galaxies: stellar content – galaxies: statistics

1. Introduction

Barred galaxies are the dominant type among spirals. In the *Third Reference Catalogue of Bright Galaxies* (de Vaucouleurs, de Vaucouleurs & Corwin 1991), one in every three spirals has a bar. Bars play an important role for instance in the formation of the spiral structures and in favouring the presence of ring-like structures (Schwarz 1981, 1984, 1985). It is also well known that non-axisymmetric structures are at least partly responsible for supplying gas to the nuclei of the galaxies (Arsenault 1989; Quillen et al. 1995).

In recent decades, a number of photometric studies on the morphology of bars have been carried out (see, among others, Martin 1995; Ohta et al. 1990; Elmegreen & Elmegreen 1985). Determining the structure of barred galaxies is an important step towards a better understanding of their implications in the dynamics of galaxies. In particular knowledge of bar structure can help us to understand the pattern of resonances.

To fit the resonances in a spiral galaxy is a difficult issue that has not been completely resolved yet. The existence of resonances is a prediction of the density wave theory and one of its main observational tests.

Many attempts have been made to measure the location of resonances in spiral galaxies (see Elmegreen 1996 for a review). For instance, Tremaine & Weinberg (1984) did a theoretical calculation in which the corotation radius (CR) was fitted assuming that the luminosity density of particular tracers (stars or neutral hydrogen) obeyed a continuity equation. Among observational studies, we may mention the paper by Cepa & Beckman (1990), who measured the CR by studying the SFR in the arm and inter-arm regions of a spiral galaxy. Elmegreen & Elmegreen (1990) and Elmegreen, Elmegreen & Montenegro (1992) determine the CR and other resonances by analysing observational structures such as rings of star formation, spurs, etc., structures that are recovered by studying the symmetry patterns. Recently, Puerari & Dottori (1997) developed a method for determining the CR based on the phase patterns in B-band and I-band photometric disc images. This method was applied to a sample of ten barred spirals by Aguerri et al., (1998) and one of the galaxies of the present paper (NGC 7479) was studied by Puerari & Dottori (1997).

In this paper, we study the photometric structure of three barred galaxies: NGC 1300, NGC 7479 and NGC 7753. We have determined the structural parameters (radial length and strength) for the bars of these galaxies. We have also studied common features in the $B-I$ and $B-V$ colour-index profiles, which allow us to infer the location of the CR for the galaxies.

2. Observations and target objects

The barred galaxies NGC 1300, NGC 7479 and NGC 7723 were observed during 1990 August at the Cassegrain focus of the 2.5 m Isaac Newton Telescope at the Roque de los Muchachos Observatory, La Palma. A GEC6 CCD was used. The pixel size imposes a theoretical limit of $0.54''$ on the angular resolution on the sky. The seeing conditions gave a practical limit of about $1''$ in spatial resolution. The detector area was 385×578 pixel. The field, limited by the chip size, was $3.47' \times 4.30'$. In the analysis presented here broad-band B, V and I images were used.

Standard routines from IRAF were used to bias-correct and flat-field the images. The sky level was subtracted using star-free

Send offprint requests to: J.A.L. Aguerri

regions well away from the galaxy images, and field stars and cosmic ray bright points were removed. Images were corrected for inclination and dust extinction by our Galaxy.

In Fig. 1 we present B- and I-band images of the sample. For all plots north is up and east is to the left. Images have been smoothed with a Gaussian filter with $\sigma = 0.7''$.

A detailed description of the data reduction process is given in Aguerri et al. (2000), which includes an extensive photometric analysis of a large sample of spirals.

For the purpose of the discussion that follows we give here a brief description of each of the galaxies in our sample.

NGC 1300 is an SBbc galaxy (de Vaucouleurs et al. 1991). Photometric studies have been carried out for this galaxy by, for example, Borkhead & Borgess (1973) and Baumgart & Peterson (1986). Dynamical models have been made by England (1989) and Lindblad & Kristen (1996). It is possible to see in the B-band image shown in Fig. 1 that the galaxy presents two dust patches starting at the nucleus and aligned with the bar. Also obvious are the very prominent and large spiral arms, which begin at the end of the bar and twist into a nearly complete circle (see Fig. 1).

NGC 7479 is the latest-type galaxy of our sample. It is classified as SB(s)c by de Vaucouleurs et al. (1991), and has a LINER nucleus (Keel 1983). Many photometric studies of this galaxy have been performed (Benedict 1982; Blackman 1983; Baumgart & Peterson 1986). NGC 7479 has a very prominent bar and non-symmetric spiral arms, the northern one being patchy, or broken. As is clearly seen in the B-band image, the dust distribution is quite complex (see Fig. 1).

NGC 7723 is catalogued as SB(r)b (de Vaucouleurs et al. 1991). In the B-band image it is possible to discern two dust patches emerging from the centre and following the direction of the bar, as in the case of NGC 1300. This galaxy has a pseudo-ring at the end of the bar (see Fig. 1).

3. Structural parameters of the bars

In this section we shall determine the structure of the bars for the galaxies NGC 1300, NGC 7479 and NGC 7723 as defined by their lengths and strengths. A very good review of these properties in barred galaxies can be found in Ohta (1996). These parameters will be obtained from the I-band images of the galaxies. This is less affected by dust extinction than optical bands and is a better tracer of the mass distribution in the galaxies.

3.1. Length of the bars

An important parameter, which will later be used for fitting the resonances, is the length of the bar. There are various methods for measuring a bar's length; for example, the isophotal fitting with ellipses (Wozniak & Pierce 1991; Wozniak et al. 1995) or the Fourier analysis of azimuthal luminosity profiles (Ohta et al. 1990). In what follows we shall concentrate on the latter.

The starting point of the method are the azimuthal luminosity profiles and their Fourier decomposition. For this purpose we have first deprojected the broad-band images of the galaxies (taking as inclination values 48.6° for NGC 1300, 40.6° for NGC 7479 and 47.46° for NGC 7723, de Vaucouleurs et al. 1991) and then we have decomposed the deprojected profiles, $I(r,\theta)$, into a Fourier series:

$$I(r,\theta) = A_0(r)/2 + \sum \big(A_m(r)\cos(m\theta) + B_m(r)\sin(m\theta)\big), \quad (1)$$

where the coefficients are given by:

$$A_m(r) = 1/\pi \int_0^{2\pi} I(r,\theta)\cos(m\theta)d\theta \quad (2)$$

and

$$B_m(r) = 1/\pi \int_0^{2\pi} I(r,\theta)\sin(m\theta)d\theta. \quad (3)$$

The Fourier amplitude of the m-th component is defined by the expressions

$$I_0(r) = A_0(r)/2 \quad (4)$$

and

$$I_m(r) = (A_m^2(r) + B_m^2(r)). \quad (5)$$

In Fig. 2 we present the relative Fourier amplitudes, I_m/I_0 ($m = 1, 2, ..., 6$), as a function of galactocentric distance in the I bandpass for each galaxy.

In the bar region it is observed that the even components are dominant. In particular the $m = 2$ component is the most remarkable in all cases. Odd components are smaller than the even ones. The values of odd components indicate the symmetry of the bar: when the bar is non-symmetric these components are important.

Aguerri et al. (1998) determined the bar radius as the point at which the odd components of the Fourier analysis begin to increase. This method has some ambiguity in some cases. Ohta et al. (1990) determined the bar's length by studying the luminosity contrasts between the bar and interbar intensity as a function of radial distance. In Fig. 3 we represent this contrast taking $I_0 + I_2 + I_4 + I_6$ as the intensity of the bar ($I_{\rm b}$) and $I_0 - I_2 + I_4 - I_6$ as the interbar intensity ($I_{\rm ib}$). The bar region is defined as the zone with a contrast exceeding 2.0, i.e. $I_{\rm b}/I_{\rm ib} > 2$. So we can determine two distances unambiguously; the first one at $I_{\rm b}/I_{\rm ib} = 2$ is called the inner radius, $R_{\rm in}$, and the second one the outer radius, which is the radius of the bar, $R_{\rm b}$. We have used the I-band images to obtain $R_{\rm b}$.

A fixed ratio,($I_{\rm b}/I_{\rm ib}$), to define the bar region would not take into account the wide variety of bar luminosities present in barred galaxies, as can be seen in Fig. 3, where the shape of the curve I_b/I_{ib} is different for each galaxy. In order not to make a poor identification, the precise shape of the curve $I_{\rm b}/I_{\rm ib}$ has to be considered. We then propose a method that takes into account the shape of the curve I_b/I_{ib} in the definition of the bar zone. We define the bar zone as follows:

$$(I_{\rm b}/I_{\rm ib}) > \frac{(I_{\rm b}/I_{\rm ib})_{\rm max} - (I_{\rm b}/I_{\rm ib})_{\rm min}}{2} + (I_{\rm b}/I_{\rm ib})_{\rm min}. \quad (6)$$

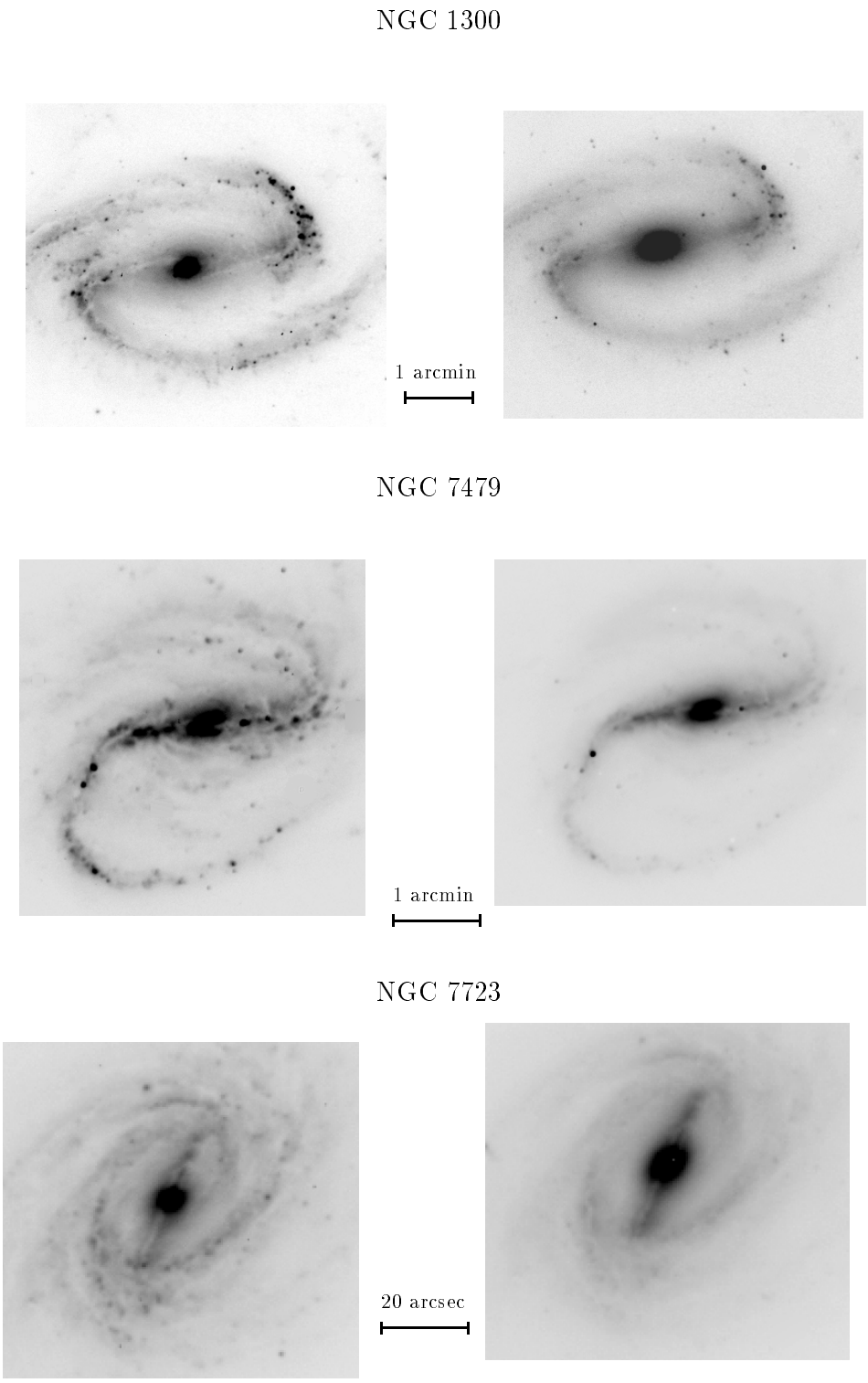

Fig. 1. B- (left) and I- (right) band images of the galaxies. North is to the right and east is up in all the figures.

This is equivalent to taking the full width at half maximum of the curve $I_{\rm b}/I_{\rm ib}$. In Table 1 we give the results derived for our sample. This criterion allows low surface brightness bars, for which Ohta et al. (1990) method fails, to be taken into account.

As mentioned previously, other techniques have been used to measure the bar length. Wozniak & Pierce (1991) and Wozniak et al. (1995) used the ellipticity of the isophotes. They take

Table 1. Structural parameters for the bars of NGC 1300, NGC 7479 and NGC 7723 in the I band

Galaxy	$S_{\rm b}$	$R_{\rm b}(''$)
NGC 1300	0.37	87
NGC 7479	0.53	63
NGC 7723	0.18	23

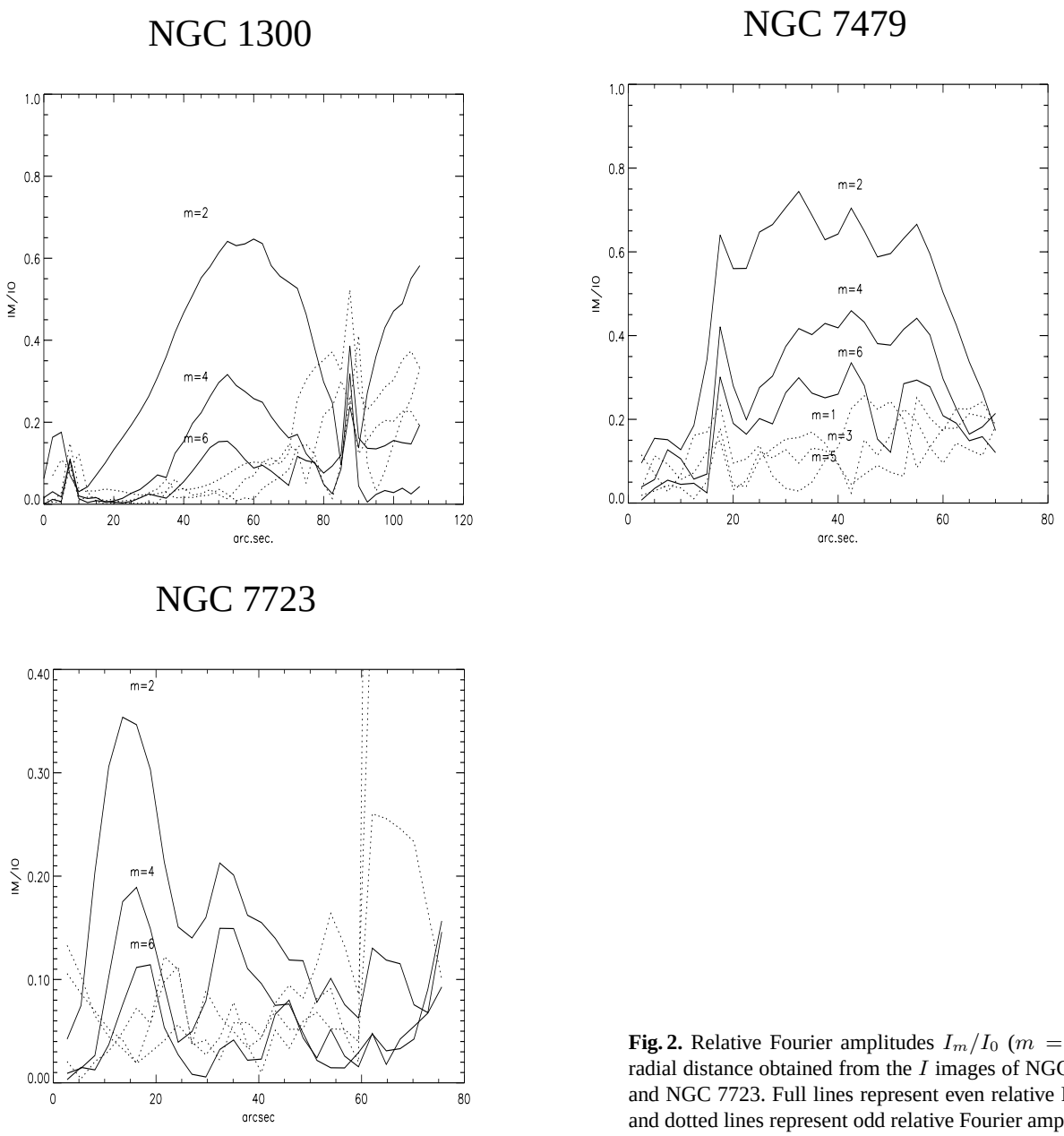

Fig. 2. Relative Fourier amplitudes I_m/I_0 ($m = 1, 2, ..., 6$) versus radial distance obtained from the I images of NGC 1300, NGC 7479 and NGC 7723. Full lines represent even relative Fourier amplitudes and dotted lines represent odd relative Fourier amplitudes.

the bar length at the maximum of the ellipticity ($e_{\max}$) or at the first minimum on the ellipticity profile ($e_{\min}$) just after the maximum. The isophotal study of the three barred galaxies of the present study is presented in Aguerri et al. (2000). We have used those ellipticity profiles to measure the bar length. The results are given in Table 2. It may be noted that our bar lengths are always between the lengths obtained using the maximum and minimum ellipticity methods.

Visual criteria are also useful to measure the bar length. Martin (1995) defines the semi-major axis of the bar as the length from the galaxy centre to the sharp outer tip where spiral arms begin. He estimate that with his method the uncertainty is about 20%. One of our galaxies, NGC 7479, is included in Martin's paper. He obtained a bar semi-length of $57''$. Chapelon et al. (1999) have proposed a more automatic visual method.

Table 2. Bar lengths (in arcsec) obtained from ellipticity methods ($e_{\min}, e_{\max}$) and the Chapelon et al. (1999) method.

Galaxy	$e_{\max}$	$e_{\min}$	Chapelon et al. (1999)
NGC 1300	83.5	122.2	85
NGC 7479	48.3	94.2	57
NGC 7723	18.2	29.2	21

They first extract a photometric profile along the major axis of the bar. They then define the semi-major axis of the bar as the distance from the centre of the galaxy to where the slope surface brightness profile steepens abruptly. None of galaxies in our sample is included in the Chapelon et al. (1999) sample,

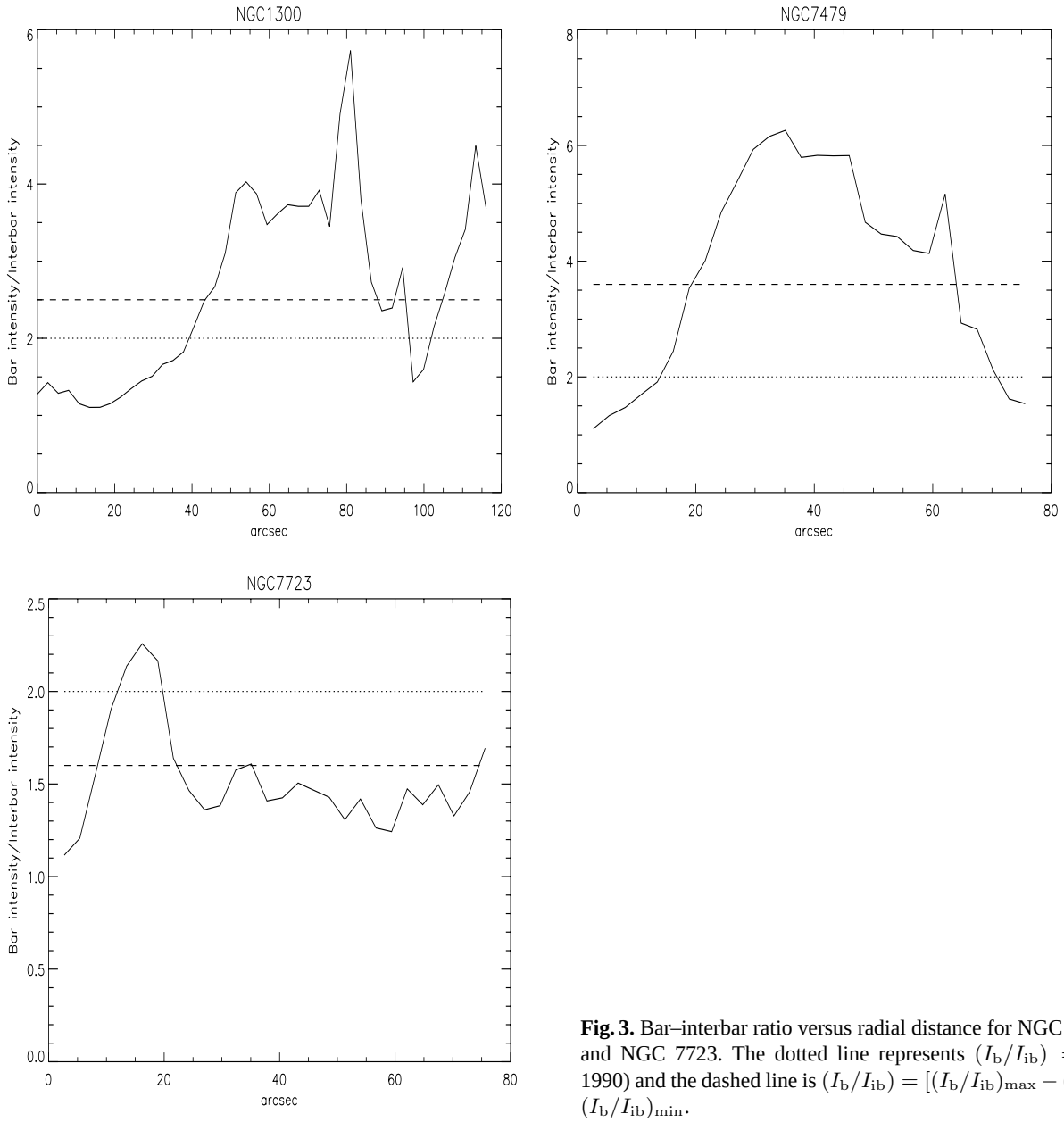

Fig. 3. Bar–interbar ratio versus radial distance for NGC 1300, NGC 7479 and NGC 7723. The dotted line represents $(I_{\rm b}/I_{\rm ib}) = 2$ (Ohta et al. 1990) and the dashed line is $(I_{\rm b}/I_{\rm ib}) = [(I_{\rm b}/I_{\rm ib})_{\rm max} - (I_{\rm b}/I_{\rm ib})_{\rm min}]/2 + (I_{\rm b}/I_{\rm ib})_{\rm min}$.

but we have obtained the semi-major axis length for our bars using this method. The results are given in Table 2.

The main problem with the visual methods is that they are not automatic and they rely on the subjective judgment of where the bar ends. The method using the isophotal ellipticity profiles are automatic but have also some problems, such as those pointed out by Wozniak et al. (1995). For example, this method cannot give a reliable estimate of the bar length for those galaxies with a bar and spiral arms not separated by a ring giving a clear dip in the ellipticity profile. This is the case for one of our galaxies (NGC 7479).

The method presented in this paper tries to solve some of these problems. Our method is automatic and improves the Ohta et al. (1990) criterion by taking into account low surface brightness bars. Therefore, it can be applied to those galaxies excluded by the ellipticity method. The results presented in Tables 1 and 2 show that our bar lengths are between the values given by the maximum and minimum ellipticity methods and are in good agreement with the values obtained using the Chapelon et al. (1999) method.

3.2. Strength of the bars

Following Dubath et al. (1990) the strength of the bar is defined as:

$$S_{\rm b} = 1/R_{\rm b} \int_0^{R_{\rm b}} I_2/I_0 dr, \tag{7}$$

where R_b is the radius of the bar. This parameter is a measure of the prominence of the bar in a galaxy. The results obtained for our galaxies are given in Table 1.

4. Identifying the corotation resonance in barred spiral galaxies

Lindblad resonances are those regions in which the angular velocity is given by

$$\Omega = \Omega_{\rm b} + \kappa/m, \tag{8}$$

where $\Omega_{\rm b}$ is the pattern speed of the density wave and κ is the epicyclic frequency (Binney & Tremaine 1987):

$$\kappa^2 = (2\Omega)^2[1 + (r/2\Omega)(d\Omega/dr)]. \tag{9}$$

The orbits in a bar potential differ from those in a disc potential. The stability criteria of periodic orbits in a bar potential (Contopoulos et al. 1989) predict that in a barred galaxy the CR cannot be located within the bar region, but has to be at the end of the bar or beyond. Moreover, in studying the dust lanes in galactic bars, Athanassoula (1992) has said that the CR has to lie in the interval $(1.2 \pm 0.2)R_{\rm b}$.

It is difficult to determine the CR from observations. The most successful methods are kinematical ones, but as a first approximation photometry is also useful. Our aim is to find some common features at the CR in the colour profiles for the three barred galaxies considered in this paper.

4.1. A photometric determination of the CR

According to the spiral density wave (SDW) theory, a non-axisymmetric perturbation induced in a different rotating disc should produce a quasi-stationary spiral wave that rotates with constant angular speed, $\Omega_{\rm p}$. At the CR the material of th e disc, in its differential rotation, equals the pattern speed. If we consider the component of the difference between rotational speed and pattern speed projected perpendicular to an arm of pitch angle i, the condition that a shock may be produced at a given radius R is (Cepa & Beckman 1990) $|\Omega - \Omega_{\rm p}|\ R\ \sin i > v_{\rm s}$, where $v_{\rm s}$ is the sound speed in the interstellar medium. The last equation is not satisfied, and neither is the gas shocked, at the CR (but it can be shocked before and after the CR). This implies that we can expect an older stellar population at the CR than in the surroundings. In an observational paper, Cepa & Beckman (1990) studied the relative arm/interarm star formation efficien cy and they locate the CR at its minimum.

There are, however, some limitations on the use of the SDW theory. This is a linear theory in which self-gravity of the gas is neglected and the non-axisymmetric perturbations must be weak to allow the linearization of the equations. Other results coming from hydrodynamical simulations (e.g. Athanassoula 1992) show that the shear can be so high in shocks that the time scale for the disruption of molecular clouds could be shorter than the time scale for collapse. Thus, star formation could be inhibited in shocks, at least for the strongest ones.

We propose here a method based in the assumptions of Cepa & Beckman (1990). This method take into account the age of the stellar population along the bar major axis.

In order to identify this older stellar population we have used the $B-I$ and $B-V$ azimuthal colour-index profiles. These profiles are shown in Fig. 4 and were obtained from the isophote fitting. The errors shown in these profiles are of two different types. The error bars represent the errors produce by the fit of the galactic isophotes by ellipses. This fit was made using the program ELLIPSE from the IRAF package. The errors due to the sky background subtraction are represented by dashed lines in Fig. 4, they were computed following Silva & Elston (1994).

Table 3. $B-I$ and $B-V$ colours measured in dust-free extinction regions of the galaxies

Galaxy	Galactocentric distance (“)	$B-I$	$B-V$
NGC 1300	90	1.42 ± 0.05	0.49 ± 0.04
	100	1.42 ± 0.06	0.46 ± 0.03
	110	1.39 ± 0.04	0.51 ± 0.03
NGC 7479	63	1.55 ± 0.09	0.57 ± 0.06
	66	1.36 ± 0.11	0.51 ± 0.09
	71	1.36 ± 0.08	0.45 ± 0.09
	75	1.32 ± 0.09	0.48 ± 0.07
NGC 7723	23	1.86 ± 0.08	0.74 ± 0.02
	28	1.67 ± 0.04	0.63 ± 0.63
	31	1.64 ± 0.03	0.62 ± 0.02
	40	1.58 ± 0.04	0.60 ± 0.03

Our assumptions are that the CR is located in the interval $(1.2 \pm 0.2)R_{\rm b}$ and at this point an old stellar population (compared with the surroundings) is expected. So we shall focus our attention on red regions located in the interval $(1.2 \pm 0.2)R_{\rm b}$. These points were selected from the $B-I$ and $B-V$ colour-index profiles.

In order to avoid reddening by dust extinction, we have measured the colours of these selected regions directly on the images. We did this by taking apertures of 5×5 pixels in regions with no visible dust extinction and located in the bar major-axis direction. The values of the colours given in Table 3 and in the colour–colour diagrams of Fig. 4 are the mean colours obtained from several of these apertures located at the same galactocentric distance and on both sides of the bar.

In order to know which point represents the oldest stellar population, we have plotted the colour–colour $B-V$ vs. $B-I$ diagrams in Fig. 4. We have also included for comparison a set of population synthesis models by Vazdekis et al. (1996), for single-burst stellar populations, for a bimodal Salpeter type IMF, for different ages and three different metallicities: $Z = 0.008$ (solid line), $Z = 0.02$ (dotted line) and $Z = 0.05$ (dashed line) (see Vazdekis et al. 1996, for more details). The results found are the following:

NGC 1300: The end of the bar is at about $87''$. As we can see in Fig. 4, the region between $90''$ and $110''$ has an almost constant colour followed by a prominent blue peak due to the beginning of the spiral arms. We have measured the $B-I$ and $B-V$ colours in regions free from dust extinction at $90''$, $100''$ and $110''$. The colour of these three regions is compatible with a stellar population of similar age and metallicity (see F igure 4), so the CR could be anywhere within this region. We fix the CR at the median point of this interval, i.e. at $100'' \pm 10''$, although

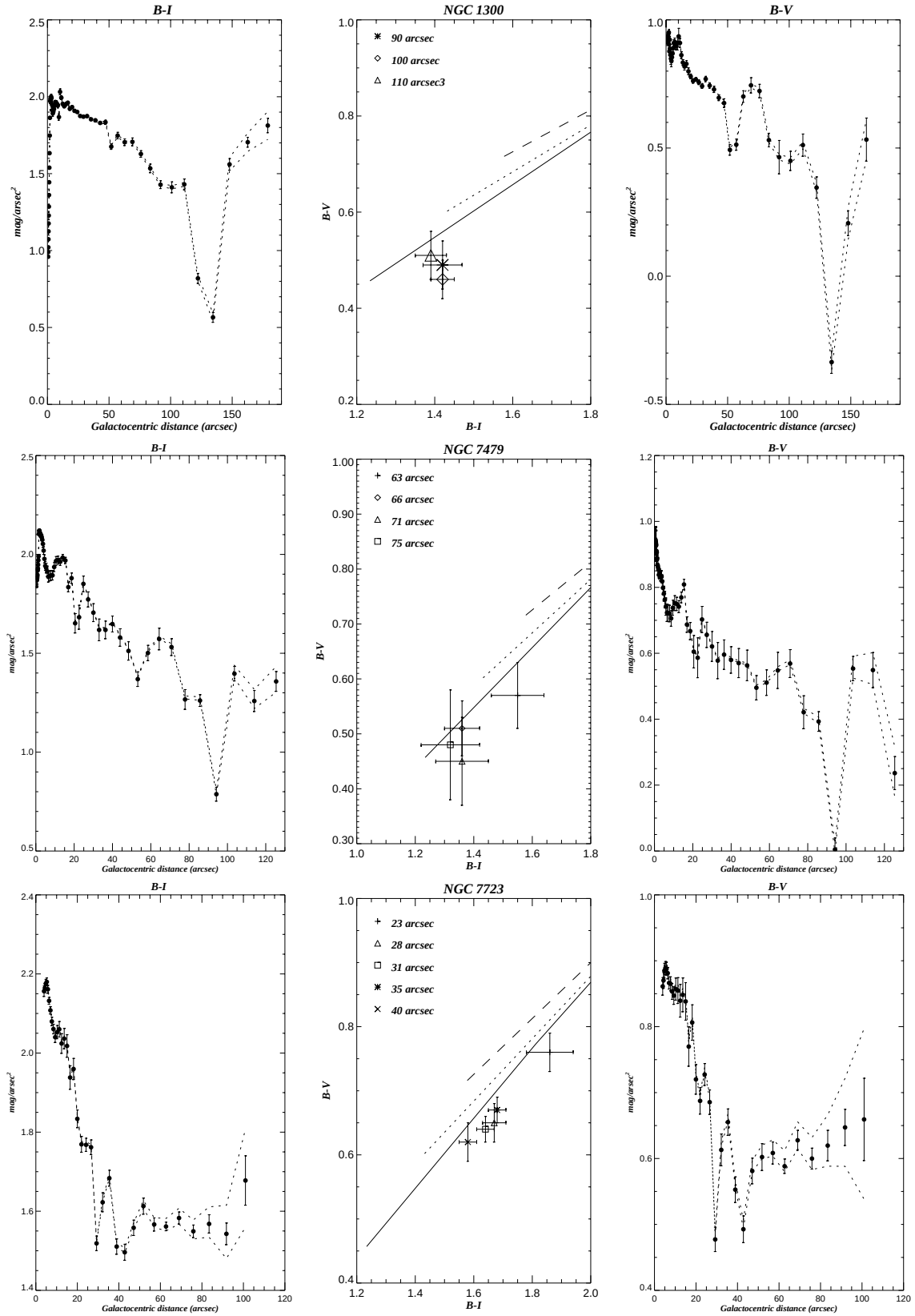

Fig. 4. $B-I$ (left) and $B-V$ (right) colour-index profiles from isophotal fitting of NGC 1300, NGC 7479 and NGC 7723. Colour–colour diagram $B-V$ vs. $B-I$ (middle) of some selected regions of NGC 1300, NGC 7479 and NGC 7723. Errors bars of the index profiles represent errors from the ellipse fitting and the dashed line are errors from the sky background subtraction. In the colour-colour diagram are also overplotted the colours given by the stellar population synthesis models of Vazdekis et al. (1996) for different metallicities and ages. In these plots the youngest stellar populations are located on the left-hand side of the diagrams (see text for more details).

Table 4. $R_{\rm CR}$ and $R_{\rm b}$ for NGC 7479 obtained from the literature

Reference	$R_{\rm CR}('')$	$R_{\rm b}('')$
Duval & Monet (1989)	56	56
Beckman & Cepa (1990)	56	56
del Rio & Cepa (1998)	85	59
Elmegreen & Elmegreen (1985)	74–106	
Quillen et al. (1995)	45	45
Sempere et al. (1995)	57	
Laine (1996)	55	45
Puerari & Dottori (1997)	55	

our method cannot give us the exact position of the CR. The gas simulation made by England (1989) predicts that the CR of this galaxy is located just at the end of the bar (83″). Later simulations (Linblad and Kristen 1996) proposed a CR at 105″ and the value given by Elmegreen & Elmegreen (1985) is 101″ for the CR. These values are in a good agreement with our value.

NGC 7479: The end of the bar is at a galactocentric distance of about 63″. At this distance a red zone surrounded by two blue ones can be identified in the $B-I$ and $B-V$ colour-index profiles. We have selected regions with galactocentric distances of 63″, 66″, 71″ and 75″ (see Fig. 4). The region located at 63″ shows an older stellar population than the other three regions. Therefore, we fix the CR at this galactocentric distance.

This galaxy has been extensively studied by other authors. Table 4 shows the values of the CR given by other authors. The CR is located within the interval 45″–106″. But most of the results are within the interval 55″–57″. This position of the CR is in very good agreement with our result and is even better when we consider the errors of these measurements. For example, Sempere et al. (1995) and Laine (1996) used a similar technique for getting the CR, they match the simulation results to observations. The simulations made by Laine (1996) give a pattern speed of $\Omega_{\rm p} = 27 \pm 3\,{\rm km\,s^{-1}\ kpc^{-1}}$. The error in the pattern speed gives an error of about 6–7″ in the CR. This error is even greater in Sempere et al. (1995), their error in $\Omega_{\rm p}$ being $\pm 5\,{\rm km\,s^{-1}\ kpc^{-1}}$. This means that our value of 63″ is in the interval, within the error, of the values given by those simulations. The CR predicted by del Rio & Cepa (1998) implies a $\Omega_{\rm p} = 100\,{\rm km\,s^{-1}\ kpc^{-1}}$. This is a very different $\Omega_{\rm p}$ from those given by the simulations.

NGC 7723: The bar finishes at 23″. There is a constant-colour region from the end of the bar until ∼27″ follow by a blue peak in the $B-I$ colour-index profile. We have taken the colours of regions with galactocentric distances of 23″, 28″, 31″, 35″ and 40″ (see Fig. 4). The oldest stellar population is located at 23″. So the CR should be located at this point. This galaxy was studied by del Rio & Cepa (1998). The semi-major axis length of the bar is the same as that presented here but they locate the CR at 35″. We hav e also measured the colours at these points, and the stellar population deduced is not different from the other locations. It is only at 23″ where the colours are compatible with an older stellar population.

5. Summary

We have studied the barred galaxies NGC 1300, NGC 7479 and NGC 7723. In the first part of the paper we concentrate on their bars, studying their lengths and strengths. For this we have used azimuthal radial profiles and their decomposition into Fourier series. For each azimuthal profile we have studied the bar–interbar intensity ratio, $(I_{\rm b}/I_{\rm ib})$. It is shown that to define the bar region as the zone in which $(I_{\rm b}/I_{\rm ib}) > 2$, as has been done in previous studies, without taking the luminosity of the bar into account, may result in a poor identification. In this paper we find it more realistic to define the bar region as that which follows $(I_{\rm b}/I_{\rm ib}) > [(I_{\rm b}/I_{\rm ib})_{\rm max} - (I_{\rm b}/I_{\rm ib})_{\rm min}]/2 + (I_{\rm b}/I_{\rm ib})_{\rm min}$.

In the second part of the paper we have studied some common features in the $B-I$ colour index profiles that can help us to locate the CR for these galaxies. Two important characteristics of the CR should be taken into account: a) the CR is located at the end or beyond the end of the bar and b) the CR should be a region lacking in star formation. We can then expect an older stellar population at the CR than in its surroundings. Using $B-I$ and $B-V$ colour-index profiles, we can select those points with red colours in the region $(1.2 \pm 0.2)R_{\rm b}$. In order to avoid dust extinction, we have measured the $B-I$ and $B-V$ colours directly in the images in regions of 5×5 pixels free of dust extinction. These colours were compared with a set of population synthesis models by Vazdekis et al. (19 96). The results are that $R_{\rm CR} \sim 100'' \pm 10''$ for NGC 1300, $R_{\rm CR} \sim 63''$ for NGC 7479 and $R_{\rm CR} \sim 23''$ for NGC 7723, values which are in agreement with those previously reported in the literature, which demonstrates the utility of accurate photometry for this kind of observation.

Acknowledgements. The Isaac Newton Telescope is operated on the island of La Palma by the Royal Greenwich Observatory at the Spanish Observatorio del Roque de los Muchachos of the Instituto de Astrofísica de Canarias. This work has been partially supported by The Spanish DGES (Direción General de Enseñanza Superior) Grant No PB97-0158. We acknowledge the editor of A&A for his great help. We also acknowledge our referee (Dr. Wozniak) for his careful reading of the paper and for his useful com ments. Thanks are due to the IAC's Scientific Editorial Service for linguistic and stylistic corrections to the text.

References

Aguerri J.A.L., Beckman J.E., Prieto M., 1998, AJ 116, 2136
Aguerri J.A.L., Varela A.M., Prieto M., Muñoz-Tuñón C., 2000, AJ, in press
Arsenault T.R., 1989, A&A 217, 66
Athanassoula E., 1992, MNRAS 259, 345
Baumgart C.W., Peterson C.J., 1986, PASP 98, 56
Beckman J.E., Cepa J., 1990, A&A 229, 37
Benedict G.F., 1982, AJ 87, 76
Binney J., Tremaine S., 1987, In: Galactic Dynamics. Princeton Univ. Press, Princeton, p. 121
Blackman C.P., 1983, MNRAS 202, 379
Borkhead M.S., Borgess R.D., 1973, AJ 78, 606
Cepa J., Beckman J.E., 1990, ApJ 349, 497
Chapelon S., Contini T., Davoust E., 1999, A&A 345, 81

Contopoulos G., Gottesman S.T., Hunter J.H., England M.N., 1989, ApJ 343, 608
del Rio S., Cepa J., 1998, A&A 340, 1
de Vaucouleurs G., de Vaucouleurs A., Corwin M.G., 1991, Third Reference Catalogue of Bright Galaxies. Springer, New York
Dubath P., Jarvis B.J., Martinet L., Pfenniger D., 1990, In: Busarello G., Capaccioli M., Longo G. (eds.) Morphological and Physical Classification of Galaxies. Kluwer, Dordrecht, p. 461
Duval M.F., Monnet G., 1985, A&AS 61, 141
Elmegreen B.G., Elmegreen D.M., 1985, ApJ 288, 438
Elmegreen B.G., Elmegreen D.M., 1990, ApJ 355, 52
Elmegreen B.G., Elmegreen D.M., Montenegro L., 1992, ApJS 79, 37
Elmegreen B.G., 1996, In: Buta R., Crocker D.A., Elmegreen B.G. (eds.) Barred Galaxies. IAU Colloquium 157, ASP Conf. Ser. vol. 91, ASP, San Francisco, p. 197
England M.N., 1989, ApJ 344, 669
Keel W.C., 1983, ApJ 268, 632
Laine S.J., 1996, Ph.D. Thesis, Florida University
Lindblad P.A.B., Kristen H., 1996, A&A 313, 733
Martin P., 1995, AJ 109, 2428
Ohta K., Masaru H., Wakamatsu K., 1990, ApJ 357, 71
Ohta K., 1996, In: Buta R., Crocker D.A., Elmegreen B.G. (eds.) Barred Galaxies. IAU Colloquium 157, ASP Conf. Ser. vol. 91, ASP, San Francisco, p. 44
Puerari I., Dottori H., 1997, ApJ 476, L73
Quillen A.C., Frogel J.A., Kenney J.D.P., Pogge R.W., Depoy D.L., 1995, ApJ 441, 549
Sempere M.J., Combes F., Casoli F., 1995, A&A 299, 371
Schwarz M.P., 1981, ApJ 247, 77
Schwarz M.P., 1984, MNRAS 209, 93
Schwarz M.P., 1985, MNRAS 212, 677
Silva D.R., Elston R., 1994, ApJ 428, 511
Tremaine S., Weinberg D.M., 1984, ApJ 282, L5
Vazdekis A., Casuso E., Peletier R.F., Beckman J.E., 1996, ApJS 106, 307
Wozniak H., Friedli D., Martinet L., Martin P., Bartschi P., 1995, A&AS 111, 115
Wozniak H., Pierce M.J., 1991, A&AS 88, 325